

# Supporting Information

## Construction of RNA-Quantum Dot Chimera for Nanoscale Resistive Biomemory Application

*Taek Lee<sup>1</sup>, Ajay Kumar Yagati<sup>2</sup>, Fengmei Pi<sup>1</sup>, Ashwani Sharma<sup>1</sup>, Jeong-Woo Choi<sup>2,\*</sup> and  
Peixuan Guo<sup>1,\*</sup>*

<sup>1</sup>Nanobiotechnology Center, Markey Cancer Center, and Department of Pharmaceutical Sciences, University of Kentucky, Lexington, KY 40536, USA.

<sup>2</sup>Department of Biomedical Engineering, Gachon University, 191 Hambakmoero, Yeonsu-gu, Incheon, 406-799, Republic of Korea.

<sup>3</sup>Department of Chemical and Biomolecular Engineering, Sogang University, 35 Baekbeom-ro (Sinsu-dong), Mapo-gu, Seoul 121-742, Republic of Korea.

### ***Design and sequence information of pRNA-3WJ-c harboring Sephadex aptamer***

The sequence information of the pRNA-3WJ-c which harbor the sephadex aptamer was obtained from a previous report.<sup>1,2</sup> The Sephadex aptamer-tagged pRNA-3WJ-c (SEPapt-3WJ-c) strand was synthesized by *in vitro* transcription of corresponding DNA template by T7 RNA polymerase. Table S.1 shows the DNA template and forward primer, reverse primer information.

### ***The Surface Investigation of pRNA-3WJ, Qd/STV, Qd/STV/Bio-3WJ-SH Conjugate by STM***

To investigate the surface morphologies and roughness of conjugated Qd/STV/Bio-3WJ-SH chimera, STM measurement was carried out. For this one, the pRNA-3WJ, Qd/STV and Qd/STV/Bio-3WJ-SH chimera were self-assembled on Au surface, respectively. In case of the pRNA-3WJ molecule, small bar types of pRNA-3WJ were well adsorbed onto the Au substrate (Figure S.1a). The vertical molecular size is around  $4.874 \pm 0.371$  nm. However, the surface of Qd/STV adsorbed on Au showed the globular shape and different vertical size compared to pRNA-3WJ molecule. The vertical size of the Qd/STV molecule was around  $17.349 \pm 1.213$  nm (Figure S.1b). The Qd/STV molecules were larger than the pRNA-3WJ molecule. The shape of Qd/STV/Bio-3WJ-SH chimera was shown in Figure S.1c. vertical molecular size is around  $21.338 \pm 0.883$  nm. Also, the shape is little different from Qd/STV and pRNA-3WJ. As a result, the Qd/STV/Bio-3WJ-SH hybrid nanoparticle was well prepared.

Moreover, the surface roughness values of pRNA 3WJ, Qd/STV and Qd/STV/Bio-3WJ-SH conjugate nanoparticle were analyzed, respectively, by provided AFM Nanoscope software (Figure S.1d). In case of the pRNA-3WJ molecules, the  $R_a$  value is  $0.387 \pm 0.231$  nm and RMS roughness ( $R_q$ ) shows  $1.784 \pm 0.611$  nm,  $R_{max}$  is  $2.195 \pm 1.213$  nm. And, in

case of the Qd/STV molecules, the  $R_a$ ,  $R_q$ ,  $R_{max}$  are  $1.838 \pm 0.414$  nm,  $7.368 \pm 0.720$  nm,  $7.171 \pm 2.264$  nm, respectively. In case of the Qd/STV/Bio-3WJ-SH chimera, it is clear that the each roughness values are similar to Qd/STV molecule. the  $R_a$ ,  $R_q$ ,  $R_{max}$  are  $1.229 \pm 1.177$  nm,  $6.942 \pm 0.978$  nm,  $5.448 \pm 2.224$  nm, respectively. Based on the results, it can be concluded that the Qd/STV/Bio-3WJ-SH hybrid nanoparticle was well prepared for further experiments.

### ***Current-Distance Characteristics of the Qd/STV/Bio-3WJ-SH Hybrid Nanoparticle***

The electronic characteristics of each biomolecule hybrids were studied by recording I-s curves with a Pt/Ir tip- Qd/STV/Bio-3WJ-SH hybrid nanoparticle-Au configuration. The I-s measurements were performed by positioning the tip on top of the hybrid particle when the feedback loop was temporarily disengaged. Figure S.2 show typical I-s curves recorded for various hybrid configurations with a tunneling current ranging  $10 \text{ pA} < i_T < 5 \text{ nA}$ . The tunneling current ( $i_T$ ) increases with the decrease in distance between Pt tip and the Au surface. Because the shape of the distance-tunneling current characteristics depends on the form and magnitude of the potential barrier the tunneling current exposed (The potential barrier was assumed a rectangular). The corresponding current-distance curves showed the exponential form that result of tip-biomolecule bias was fixed at 100 mV. As shown in Figure S.3, The various electrode surfaces of the junction capacitance is decreased as the tip reaches around  $2 \text{ \AA}$ , so this junction voltage the capacitance increased exponentially however for the pRNA3WJ and Qd/STV/Bio-3WJ-SH the current raises exponentially when the tip reached around 10 and  $5 \text{ \AA}$  respectively. From Figure S.3a-c, results shows the clear presence of the molecule with an exponential decay in the tunneling current, where a plateau observed at a current  $I_w \sim 3 \text{ nA}$  and  $1.5 \text{ nA}$  attributed to the formation of a molecular connection between

the tip and the surface. There is no clear information how many particles contributed in the current, but results clearly shows that pRNA3WJ forms a molecular junction.

The analysis of the experimental data for the Qd/STV/Bio-3WJ-SH hybrid nanoparticle on Au substrate can be obtained from Figure S.3 by fitting the exponential region to measure the apparent barrier height and the conductance through the gap. The conductance through the gap can be estimated as  $G = I/e_1$  where  $e_1$  is the applied bias voltage and the apparent barrier voltage can be measured using the following equation<sup>3</sup>

$$\varphi_A(eV) = 0.952 \left( \frac{d \ln I}{dz (\text{\AA})} \right)^2$$

by fitting the exponential region of the plot yields. The values of the apparent barrier height and the conductance values are shown in Table S.2. The obtained values are in very good agreement with the distance dependence factor calculated for intermolecular two-step tunneling. Thus, our results confirms the multistep tunneling as a mechanism for intermolecular electron transfer involving the Qd/STV/Bio-3WJ-SH hybrid nanoparticle.

## References

- [1]. Y. Shu, F. Haque, D. Shu, W, Li, Z. Zhu, M. Kotb, Y. Lyubchenko, P. Guo, *RNA*, **2013**, 29, 767.
- [2]. C. Srisawat, I. J. Goldstein, D. R. Engelke, *Nucleic Acids Res.* **2001**, 29, e4.
- [3]. N. D Lang, *Phy. Rev. B*, **1998**, 37, 17.

Template	5'-GGA TCA ATC ATG GCA AAA AAG TCC GAG TAA TTT ACG TTT TGA TAC GGT TGC GGA ACT TGC-3'
Forward Primer	5'-GTA TAA TAC GAC TCA CTA TAG GGC CGG ATC AAT CAT GGC AA-3'
Reverse Primer	5'- GCA AGT TCC GCA ACC GTA TCA-3'

Table S.1 Sequence information of Sephadex aptamer-tagged pRNA-3WJ-c (SEPapt-3WJ-c)

	Thiol-modified pRNA3WJ	STV/QD	STV/QD-3WJ
<b>G (nS)</b>	<b>42</b>	<b>32</b>	<b>49</b>
<b><math>\phi_A</math> (eV)</b>	<b>0.11</b>	<b>5.1</b>	<b>0.75</b>

Table S.2 Current-distance decay factors along the barrier height of thiol-modified pRNA-3WJ, Qd/STV, Qd/STV/Bio-3WJ-SH chimera were presented, respectively.

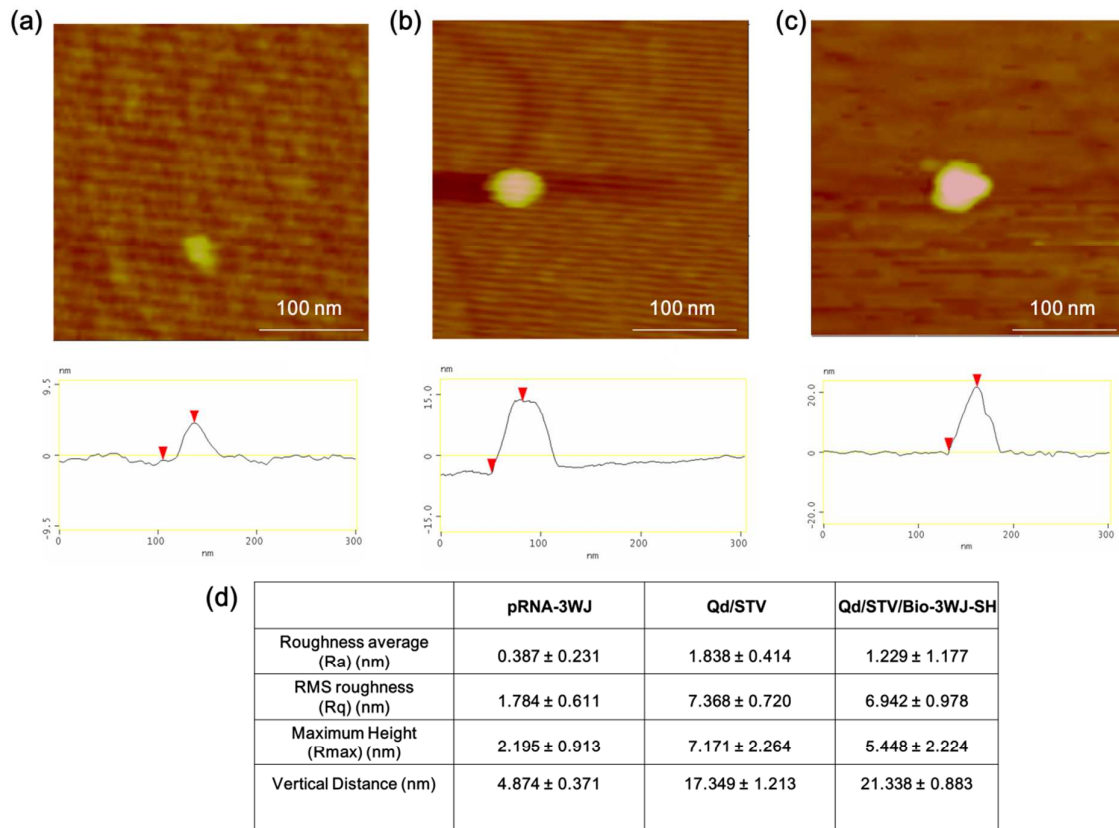


Figure S.1 AFM image of (a) Thiol-modified pRNA-3WJ, (b) Qd/STV, (c) Qd/STV/Bio-3WJ-SH chimera, (d) surface roughness analysis result.

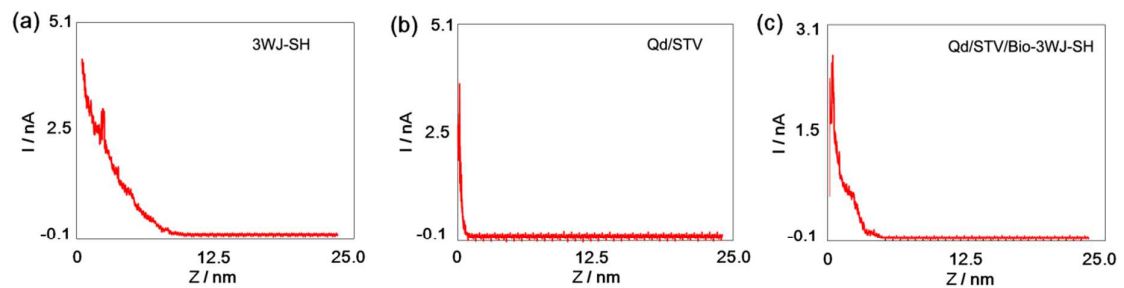


Figure S.2 Current-Distance characteristics of (a) Thiol-modified pRNA-3WJ, (b) Qd/STV (c) Qd/STV/Bio-3WJ-SH chimera.

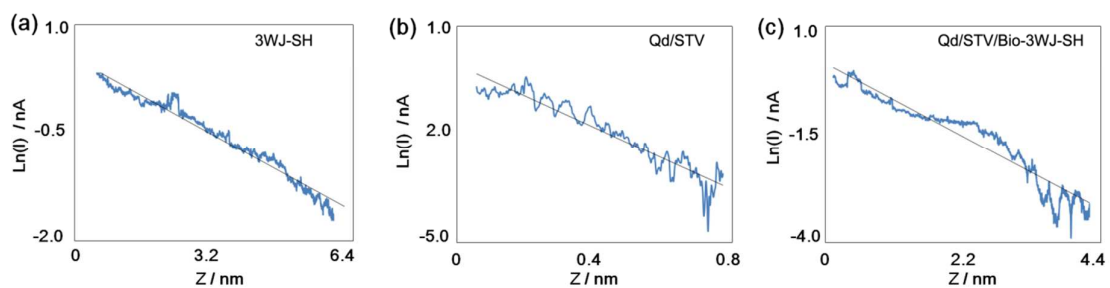


Figure S.3 Current–Distance relationship plot of  $\ln(I)$  with the tip-sample distance of (a) Thiol-modified pRNA-3WJ, (b) Qd/STV, (c) Qd/STV/Bio-3WJ-SH chimera.